Science Signaling AAAS

www.sciencesignaling.org/cgi/content/full/3/129/ra51/DC1

Supplementary Materials for

Error Minimization in Lateral Inhibition Circuits

Omer Barad, Dalia Rosin, Eran Hornstein,* Naama Barkai*

*To whom correspondence should be addressed. E-mail: naama.barkai@weizmann.ac.il (N.B.); eran.hornstein@weizmann.ac.il (E.H.)

Published 6 July 2010, *Sci. Signal.* **3**, ra51 (2010)
DOI: 10.1126/scisignal.2000857

The PDF file includes:

Section S1. Probabilistic model of lateral inhibition: rules for successful selection.
Section S2. Error rate—formal calculation.
Section S3. Error rate in a purely stochastic lateral inhibition process.
Section S4. Error rate in a lateral inhibition process with a pre-pattern bias.
Section S5. Error rate in an iterative process.
Section S6. Transcription-based feedback model of lateral inhibition process: the effective time delay, τ^{eff}.
Section S7. Cis inhibition model of lateral inhibition process: the effective time delay, τ^{eff}.
Section S8. Predicted error rates for different combinations of Notch, Delta, and Serrate heterozygotes.
Section S9. A smooth inhibition function leads to a higher error rate.
Section S10. Validation for the use of the mα reporter.
Fig. S1. Minimizing inhibition delay reduces error rate in a lateral inhibition process with a pre-pattern bias.
Fig. S2. Reduction of error rate in an iterative process.
Fig. S3. Simulation results showing the error rates as a function of the Hill coefficient.
Fig. S4. Validation of SOP detection using the mα reporter.
Table S1. Summary of the specific genotypes tested for ectopic selection of anterior scutellar (aSC) bristles.
References

Error minimization in lateral inhibition circuits:

Supplementary information

Section 1. Probabilistic model of lateral inhibition: rules for successful selection.. 2
Section 2. Error rate—formal calculation 3
Section 3. Error rate in a purely stochastic lateral inhibition process 6
Section 4. Error rate in a lateral inhibition process with a pre-pattern bias..... 7
Section 5. Error rate in an iterative process 10
Section 6. Transcription-based feedback model of lateral inhibition process: the effective time delay, τ^{eff} 11
Section 7. Cis inhibition model of lateral inhibition process: the effective time delay, τ^{eff} 16
Section 8. Predicted error rates for different combinations of Notch, Delta, and Serrate heterozygotes..... 23
Section 9. A smooth inhibition function leads to a higher error rate 25
Section 10. Validation for the use of the mα reporter 26

Section 1. Probabilistic model of lateral inhibition: rules for successful selection

In this section, we formulate a probabilistic model of a lateral inhibition process. We use this formulation to define the conditions for the successful selection of a single cell only. This leads to the derivation of Equations 1 and 3 in the main text.

As is described in the main text, we consider *n* equivalent cells and assume that they all interact with each other in an equivalent way. We further assume that each of the cells, if left uninhibited, will (1) initiate lateral inhibition, (2) become refractory to inhibition, and (3) become SOP. These processes occur at the following three times:

1. t_i^{in} : cell *i* begins to send lateral inhibition signals.
2. t_i^r : cell *i* becomes refractory to inhibition.
3. t_i^s : cell *i* is selected as SOP in an irreversible manner ($t_i^s \geq t_i^r$).

We assume that these times are stochastic variables, chosen from distributions that characterize the cell-to-cell variability (noise). We note that this formulation is valid only when the onset of these three processes is non-linear, enabling us to define such timings. Indeed, as was shown before [1, 2], non-linear interaction is essential for selection by lateral inhibition.

The communication between the cells is further characterized by two time delays. These delays define the characteristic times that elapse from the initiation of lateral inhibition by one cell, until this inhibition is felt by its counterparts. Specifically, we define:

1. $\boldsymbol{\tau}^{in}$: *inhibition delay* - the delay until the production or activity Notch ligands are inhibited.
2. $\boldsymbol{\tau}^{s}$: *selection delay* – the delay until the ability to become a SOP is inhibited.

Successful selection requires that the first cell to initiate lateral inhibition (the cell with the smallest t_i^{in} ,which we denote as cell 1) is (A) selected as SOP, and (B) represses the SOP potential of all of its neighbors, and in particular the second cell to initiate lateral inhibition (the cell with the second-smallest t_i^{in} , which we denote as cell 2). Thus, the formal conditions for successful selection are:

(A) *The selected cell (cell "1") should not be repressed by its neighbors*. This requires that either of the following two conditions is satisfied:
   I. The selected cell becomes refractory before being inhibited: $t_1^r < t_2^{in} + \boldsymbol{\tau}^s$.
   II. The selected cell prevents all other cells from sending lateral inhibition signals: $t_1^{in} + \boldsymbol{\tau}^{in} < t_2^{in}$.

(B) *None of the other cells (e.g. cell "2") will be selected*. This requires that:

$$t_1^{in} + \boldsymbol{\tau}^s < \min\left(t_2^s, t_2^r\right) = t_2^r .$$

It is convenient to define $\Delta t = t_2^{in} - t_1^{in}$, the duration of time during which only the fastest cell (cell "1") is sending lateral inhibition signals. The conditions for successful selection can then be written as:

(A) ($\Delta t > (t_1^r - t_1^{in}) - \boldsymbol{\tau}^s$ or $\Delta t > \boldsymbol{\tau}^{in}$) and (B) $\Delta t > \boldsymbol{\tau}^s - (t_2^r - t_2^{in})$.

As discussed in main text, two scenarios can be envisioned. First, if $(t_1^r - t_1^{in}) > \boldsymbol{\tau}^s$ refractoriness does not play a significant role in the selection process, and condition (B) is always satisfied. Second, when cells become refractory at about the same time as they initiate lateral inhibition [$(t_2^r - t_2^{in}) < \boldsymbol{\tau}^s$] refractoriness does play a role and only one iteration is possible. In this case, condition (A) is satisfied. In either case, we can summarize the selection rule as

(1. 1) $\Delta t > \boldsymbol{\tau}^{eff}$

Such that when $(t_1^r - t_1^{in}) >> \boldsymbol{\tau}^s$ the effective time delay $\boldsymbol{\tau}^{eff}$ given by:

(1. 2) $\boldsymbol{\tau}^{eff} = \boldsymbol{\tau}^{in}$

and in all other conditions:

(1. 3) $\boldsymbol{\tau}^{eff} = \boldsymbol{\tau}^s - (t_2^r - t_2^{in})$

To summarize, in either of the cases, successful selection following a single iteration requires that Δt be larger than some effective delay $\boldsymbol{\tau}^{eff}$, with $\boldsymbol{\tau}^{eff}$ defined as above.

Section 2. Error rate—formal calculation

In this section we use the probabilistic formulation of the lateral-inhibition process, described in section 1 above, in order to calculate the rate of erroneous selections (error-rate) in a cluster of *n* equivalent cells. Our analysis assumes that t^{in} (the time when the cell initiates lateral inhibition) is a stochastic variable, chosen at random from some distribution, which we called the "arrival time distribution". We assume a simplified

functional form for this distribution, which enables us to precisely calculate the error rate as a function of the two critical parameters: the effective time delay, $\boldsymbol{\tau}^{eff}$ and the degree of cell-to-cell variability (noise), taken here as the relative width of the arrival time distribution. Using this analysis we derive the equation describing the error rate. A special case of this equation (*n=4*) is cited by Eq. 2 in main text and Figure 3C.

Let P^{ER} denote the probability of error. Formally, P^{ER} is defined as:

(2. 1) $$P^{ER} = 1 - P\left[\left(\Delta t > \tau^{eff}\right) \cap \left(t_1^{in} < T\right)\right] = 1 - \int_o^T p\left[\left(\Delta t > \tau^{eff}\right) \cap \left(t_1^{in} = t\right)\right] dt$$

where *P* denotes probability, *p* probability density, $\Delta t = t_2^{in} - t_1^{in}$ and $\boldsymbol{\tau}^{eff}$ as defined in section 1 above. $T = \left\langle t_i^s \right\rangle$ denotes the developmental time window; if cells are not inhibited by this time, they become SOP by default.

For a cluster of *n* cells, *p* can be calculated based on $P^{AT}\left(t\right)$, the arrival time distribution:

(2. 2) $$p\left[\left(\Delta t > \tau^{eff}\right) \cap \left(t_{first}^{in} = t\right)\right] = \binom{n}{1} P^{AT}\left(t\right) P_C^{AT}\left(t + \tau^{eff}\right)^{n-1}$$

Here, $P^{AT}\left(t\right)$ denotes the probability density that one cell arrives at the threshold at a time *t* (cell arrival times are assumed to be independent), whereas the probability that a cell will arrive at some later time is given by P_C^{AT}, the complementary cumulative distribution, defined as $P_C^{AT}\left(t + \tau^{eff}\right) = \int_{t+\tau^{eff}}^{\infty} P^{AT}\left(t'\right) dt'$. The binomial coefficient indicates that any of the *n*-cells can be the first to initiate lateral inhibition.

$P^{AT}\left(t\right)$ captures the cell-to-cell variability. For simplicity (and without loss of generality), we approximate $P^{AT}\left(t\right)$ as a square function centered at the mean arrival time, $\left\langle t \right\rangle$, with a width, $\alpha\left\langle t \right\rangle$:

(2. 3) $$P^{AT}(t) = \begin{cases} 0 & t < (1-\alpha)\left\langle t \right\rangle \\ \dfrac{1}{2\alpha\left\langle t \right\rangle} & (1-\alpha)\left\langle t \right\rangle < t < (1+\alpha)\left\langle t \right\rangle \\ 0 & (1+\alpha)\left\langle t \right\rangle < t \end{cases}$$

The complementary cumulative distribution is then given by:

$$(2.4)\quad P_C^{AT}(t)=\begin{cases}1 & t<(1-\boldsymbol{\alpha})\langle t\rangle\\ \dfrac{1+\boldsymbol{\alpha}}{2\boldsymbol{\alpha}}-\dfrac{t}{2\boldsymbol{\alpha}\langle t\rangle} & (1-\boldsymbol{\alpha})\langle t\rangle<t<(1+\boldsymbol{\alpha})\langle t\rangle\\ 0 & (1+\boldsymbol{\alpha})\langle t\rangle<t\end{cases}$$

Note that α, the relative width of this distribution, can attain any value between zero and one. The case $\alpha=0$ corresponds to the deterministic dynamics (no noise) with all cells arriving at the threshold at the exact same time <t>. The case $\alpha\to 1$ corresponds to a fully stochastic process. In the latter case, the probability that a cell crosses the threshold at time *t* is uniform for all *t*<T within the developmental time window.

Substituting the $P^{AT}(t)$ (Eq. 2.3-2.4) into Eq. 2.1-2.2, we derive the error rate:

$$(2.5)\quad P^{ER}=1-\left[\left(1-\frac{\tau^{eff}}{2\alpha\langle t\rangle}\right)^n-\begin{cases}\left(\dfrac{1+\alpha}{2\alpha}-\dfrac{T+\tau^{eff}}{2\alpha\langle t\rangle}\right)^n & T<(1+\alpha)\langle t\rangle-\tau^{eff}\\ 0 & T>(1+\alpha)\langle t\rangle-\tau^{eff}\end{cases}\right].$$

For a given noise α, and effective delay τ^{eff}, we can further optimize the error rate with respect to the mean arrival time $\langle t\rangle$ to obtain the minimal error rate. This gives an optimal $\langle t\rangle$ which is of the order of the developmental time window T:

$$(2.6)\quad \langle t\rangle_{opt}=T\frac{1-\tau^{eff}/T\left(\left(\tau^{eff}/T\right)^{\frac{1}{n-1}}+1\right)}{1+\alpha\left(1-2\left(\tau^{eff}/T\right)^{\frac{1}{n-1}}\right)}\underset{\tau^{eff}/T<<1}{\approx}\frac{T}{1+\alpha\left(1-2\left(\tau^{eff}/T\right)^{\frac{1}{n-1}}\right)}$$

and a minimal error-rate (as a function of τ^{eff}, α and T):

$$(2.7)\quad P_{\min}^{ER}\approx 1-\left(1-\frac{1+\alpha\left(1-2\left(\tau^{eff}/T\right)^{\frac{1}{n-1}}\right)}{2\alpha}\frac{\tau^{eff}}{T}\right)^n$$

Thus, the minimal error rate depends on two parameters: the ratio between effective delay and developmental time window, $\frac{\tau^{eff}}{T}$, and the noise level, α. Note again that in our formalism, the development time window corresponds to the time when an un-inhibited cell is selected by default, $T = \langle t_i^s \rangle$.

Clearly, error frequency decreases with increasing randomness ($\alpha \rightarrow 1$). Assuming $n=4$, $\alpha=1$ and $\tau^{eff} << T$, we obtain the approximation given by Equation 2, main text. This function is plotted also in Figure 3C.

Section 3. Error rate in a purely stochastic lateral inhibition process

In this section we consider a purely stochastic process and derive the corresponding error rate. The difference between this case and those analyzed in Section 2 above is the function form of the arrival time distribution $P^{AT}(t)$. Specifically, in the purely stochastic process we consider an exponential, rather than a square-shape for of the arrival time distribution. We show that this case is well described by the $\alpha \rightarrow 1$ limit of the square-form analyzed above.

In a purely stochastic process, the arrival time distribution, $P^{AT}(t)$, has an exponential shape:

$$(3.\ 1) \quad P^{AT}(t) = r_k \exp^{-r_k t}$$

Substituting this in the formula for the error rate (Eqs. 2.1 and 2.2):

$$(3.\ 2) \quad P^{ER} = 1 - \mathrm{P}\left(\left(\Delta t > \tau^{eff}\right) \cap \left(t_{first}^{in} < T\right)\right) = 1 - \int_o^T \binom{n}{1} P^{AT}(t) P_C^{AT}\left(t + \tau^{eff}\right)^{n-1} dt$$

we obtain:

$$(3.\ 3) \quad P^{ER} = 1 - \int_o^T N r_k \exp^{-r_k t} \exp^{-r_k\left(t+\tau^{eff}\right)(n-1)} dt = 1 - \exp^{-r_k \tau^{eff}(n-1)}\left(1 - \exp^{-r_k T n}\right)$$

We can further optimize the arrival rate, r_k, to obtain the minimal error rate. This optimal rate is given by:

$$(3.\ 4)\quad r_{k,opt} = \frac{1}{Tn}\log\left(1+\frac{T}{\tau^{eff}}\frac{n}{n-1}\right),$$

and the corresponding minimal error rate is:

$$(3.\ 5)\quad P_{\min}^{ER} = 1-\exp\left(-\frac{\tau^{eff}}{T}\frac{n-1}{n}\log\left(1+\frac{T}{\tau^{eff}}\frac{n}{n-1}\right)\right)\left(1-\left(1+\frac{T}{\tau^{eff}}\frac{n}{n-1}\right)^{-1}\right).$$

For a typical proneural cluster of $n=4$ cells and for $\frac{\tau^{eff}}{T} << 1$ this can be approximated as

$$(3.\ 6)\quad P_{\min}^{ER} \to 1-\exp\left(-4\frac{\tau^{eff}}{T}\right) \sim 1-\left(1-\frac{\tau^{eff}}{T}\right)^{4}$$

This result is similar to the minimal error rate for the square-form approximation in the limit $\alpha \to 1$ (c.f. Eq. 2.7).

Section 4. Error rate in a lateral inhibition process with a pre-pattern bias

In this section we estimate the error rate for lateral-inhibition process in which cells are not equivalent, but are subject to some pre-pattern that biases the selection toward specific cells in the cluster. We show that the essential prediction of our analysis, namely that inhibition delay must be minimized in order to reduce selection errors, is also valid for this more general case.

We model a pre-pattern bias by assuming that different cells in the cluster are characterized by different arrival time distributions. For simplicity, we describe the analysis for a cluster of two cells, but the analysis can be easily extended to the more general case of *n* cells. Following the framework described in Section 2, we approximate the arrival time distributions characterizing the two cells by the following two square functions (see fig. S1A):

$$(4.\ 1)\quad P_1^{AT}(t) = \begin{cases} 0 & t < (1-\boldsymbol{\alpha})\langle t_1\rangle \\ \dfrac{1}{2\boldsymbol{\alpha}\langle t_1\rangle} & (1-\boldsymbol{\alpha})\langle t_1\rangle < t < (1+\boldsymbol{\alpha})\langle t_1\rangle \\ 0 & (1+\boldsymbol{\alpha})\langle t_1\rangle < t \end{cases}$$

and

$$(4.\ 2)\quad P_2^{AT}(t)=\begin{cases} 0 & t<\langle t_2\rangle-\boldsymbol{\alpha}\langle t_1\rangle \\ \dfrac{1}{2\boldsymbol{\alpha}\langle t_1\rangle} & \langle t_2\rangle-\boldsymbol{\alpha}\langle t_1\rangle<t<\langle t_2\rangle+\boldsymbol{\alpha}\langle t_1\rangle \\ 0 & \langle t_2\rangle+\boldsymbol{\alpha}\langle t_1\rangle<t \end{cases}$$

Here, we assumed that the pre-pattern bias does not affect the extent of noise, α, but introduces a difference in the mean arrival time of the two cells:

$$(4.\ 3)\quad \Delta B=\langle t_2\rangle-\langle t_1\rangle$$

Substituting these distributions in the formula for the error rate (Eq. 2.1), we obtain:

$$P^{ER}=1-\int_{\langle t_1\rangle-\alpha\langle t_1\rangle}^{\min\left(T,\langle t_2\rangle-\alpha\langle t_1\rangle-\tau^{eff}\right)}\frac{1}{2\alpha\langle t_1\rangle}dt-$$

$$(4.\ 4)\quad \int_{\min\left(T,\langle t_1\rangle+\alpha\langle t_1\rangle,\langle t_2\rangle-\alpha\langle t_1\rangle-\tau^{eff}\right)}^{\min\left(T,\langle t_1\rangle+\alpha\langle t_1\rangle,\langle t_2\rangle+\alpha\langle t_1\rangle-\tau^{eff}\right)}\frac{1}{2\alpha\langle t_1\rangle}\left(\frac{\langle t_2\rangle+\alpha\langle t_1\rangle-\left(t+\tau^{eff}\right)}{2\alpha\langle t_1\rangle}\right)^{n-1}dt-$$

$$\int_{\min\left(T,\langle t_1\rangle+\alpha\langle t_1\rangle-\tau^{eff},\langle t_2\rangle-\alpha\langle t_1\rangle\right)}^{\min\left(T,\langle t_1\rangle+\alpha\langle t_1\rangle-\tau,\langle t_2\rangle+\alpha\langle t_1\rangle-\tau^{eff}\right)}(n-1)\frac{1}{2\alpha\langle t_1\rangle}\left(\frac{\langle t_2\rangle+\alpha\langle t_1\rangle-\left(t+\tau^{eff}\right)}{2\alpha\langle t_1\rangle}\right)^{n-2}\frac{\langle t_1\rangle+\alpha\langle t_1\rangle-\left(t+\tau^{eff}\right)}{2\alpha\langle t_1\rangle}dt$$

The three integrals in this equation describe the three cases that lead to the successful selection of one cell only. The first case corresponds to a situation in which selection of the first cell is guaranteed (that is: $P_2^{AT}(t_{first}^{in}+\boldsymbol{\tau}^{eff})=0$). In the other two cases, selection occurs at times when, in principle, both cells could have been selected, that is: $P_1^{AT}(t_{first}^{in}+\boldsymbol{\tau}^{eff})>0$ and $P_2^{AT}(t_{first}^{in}+\boldsymbol{\tau}^{eff})>0$. In the second integral, the cell which is "favored" for selection (“1”) is selected, while in the third integral it is the second (“2”), non-favored cell that is selected.

The different integrals can be calculated, giving:

$$
(4.5)\quad P^{ER}=\begin{cases}
0 & \Delta B>2\alpha\langle t_1\rangle+\tau^{eff}\\
\dfrac{\Delta B-\tau^{eff}}{2\alpha\langle t_1\rangle}+\dfrac{\left(2\alpha\langle t_1\rangle\right)^n-\left(\Delta B-\tau^{eff}\right)^n}{n\left(2\alpha\langle t_1\rangle\right)^n} & \Delta B>2\alpha\langle t_1\rangle-\tau^{eff}\\
\dfrac{\Delta B-\tau^{eff}}{2\alpha\langle t_1\rangle}+\dfrac{\left(2\alpha\langle t_1\rangle\right)^n-\left(\Delta B-\tau^{eff}\right)^n}{n\left(2\alpha\langle t_1\rangle\right)^n}+\dfrac{(n-1)\left[\left(2\alpha\langle t_1\rangle\right)-\left(\Delta B+\tau^{eff}\right)\right]^n}{n\left(2\alpha\langle t_1\rangle\right)^n}-\dfrac{\Delta B\left[\left(2\alpha\langle t_1\rangle\right)-\left(\Delta B+\tau^{eff}\right)\right]^{n-1}}{\left(2\alpha\langle t_1\rangle\right)^n} & \Delta B>\tau^{eff}\\
\dfrac{\left[\left(2\alpha\langle t_1\rangle\right)-\left(\tau^{eff}-\Delta B\right)\right]^n}{n\left(2\alpha\langle t_1\rangle\right)^n}+\dfrac{(n-1)\left[\left(2\alpha\langle t_1\rangle\right)-\left(\Delta B+\tau^{eff}\right)\right]^n}{n\left(2\alpha\langle t_1\rangle\right)^n}-\dfrac{\Delta B\left[\left(2\alpha\langle t_1\rangle\right)-\left(\Delta B+\tau^{eff}\right)\right]^{n-1}}{\left(2\alpha\langle t_1\rangle\right)^n} & else
\end{cases}
$$

Equation 4.5 gives the error rates as a function of the following parameters: the initial bias (ΔB), the effective inhibition delay (τ^{eff}) and the noise level ($\boldsymbol{\alpha}\langle t_1\rangle$). It is plotted in fig. S1B. Interestingly, low error rate is obtained in two distinct domains: (1) high initial bias with respect to the noise $\Delta B>2\alpha\langle t_1\rangle$, or (2) high noise level with no, or minimal initial bias $\alpha\langle t_1\rangle >> \max\left(\Delta B,\tau^{eff}\right)$. Importantly, in both domains, decreasing the effective delay, τ^{eff} reduces the error rates (fig. S1B-C).

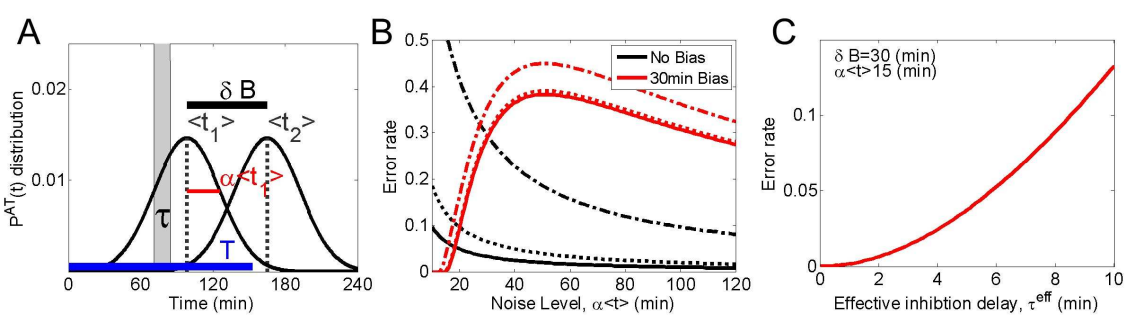

Supp Figure 1: Minimizing inhibition delay reduces error rate in a lateral inhibition process with a pre-pattern bias A) Illustration of the arrival time distributions, $P^{AT}(t)$, with initial bias of $\boldsymbol{\delta}B$ .The favored $P^{AT}(t)$ centered in $\langle t_1\rangle$ and the delayed $P^{AT}(t)$ centered in $\langle t_2\rangle$. The noise level is marked by $\boldsymbol{\alpha}\langle t_1\rangle$ (red), and the developmental time window by *T* (blue). B) Error rates as a function of the noise level for a system without initial bias (black) and a system with initial bias of 30min (red), and as a function of the effective inhibition delay: $\boldsymbol{\tau}^{eff}=\frac{1}{2},1$ and 5 min for solid, dotted and

dashdot, respectively. C) Error rates as a function of the effective inhibition delay, τ^{eff}, for biased selection with $\delta B = 30\,\text{min}$ and $\alpha\langle t_1\rangle = 15\,\text{min}$.

Section 5. Error rate in an iterative process

In sections 2-4 above, we derived the error rate for selection within a single iteration. As discussed in Section 1, when refractoriness does not play a role (due to its late onset), the system can oscillate, enabling repeated attempts for selection. In this section we calculate the overall error rate when iterations are possible ($t_2^r - t_2^{in} >> \tau^s$). We show that also in this case, low error-rate requires a short effective delay.

Because the developmental time window is finite, only a limited number of iterations are possible. For a cell that can undergo *k* iterations, the error rate is given by the probability that selection failed at all iterations:

(5. 1) $$P^{ER} = \prod_{l=1:k}\left(1 - P_l^{SC}\right),$$

where P_l^{SC} is the success rate in the lth cycle, which (assuming independent cycles) can be obtained from Eq. 2.5:

(5. 2) $$P_l^{SC} = \left(1 - \frac{\tau^{in}}{2\alpha\langle t\rangle}\right)^n - \begin{cases}\left(\dfrac{1+\alpha}{2\alpha} - \dfrac{T+\tau^{in}}{2\alpha\langle t\rangle}\right)^n & T < (1+\alpha)\langle t\rangle - \tau^{in} \\ 0 & T > (1+\alpha)\langle t\rangle - \tau^{in}\end{cases}$$

Next, we estimate the number of possible iterations. For this, we approximate the mean duration of each cycle $\langle T_c\rangle$, by adding the contributions: (1) the mean time it takes for the first cell to reach the threshold (initiate lateral inhibition) (2) the effective inhibition delay (2) and (3) the delay between cycles due to the need to degrade the inhibitory components, τ^{cycle}:

(5. 3) $$\langle T_c\rangle = \left(1 - \alpha\frac{N-1}{N+1}\right)\langle t\rangle + \tau^{in} + \tau^{cycle}.$$

The final error rate depends on the interplay between the success rate of each cycle, P_l^{SC}, and the number of possible iterations, *k*. For a given system with defined parameters, we can optimize the mean arrival time, $\langle t\rangle$ (or, equivalently, the maximal number of oscillations) in order to minimize the error rate. This minimal error rate now depends on the remaining parameters: number of cell (*n*), development time window (*T*), inhibition delay (τ^{in}), cycle delay (τ^{cycle}) and relative noise level (α).

In fig. S2 we plotted the error rate as a function of $\langle t \rangle$ for a system with the following parameters: $n = 4$, $T = 360\,\text{min}$, $\tau^{in} = 10\,\text{min}$, $\tau^{cycle} = 100\,\text{min}$ and $\alpha = 0.5$. As can be seen, the error rate can be reduced by ~3fold (from 13.2% to 4.8%) when the number of iterations are optimized. While this is a considerable improvement, it is still above the observed error rate in the flies (<1%).

We also notice that to achieve a meaningful improvement in the error rate (as is shown here), the system must show frequent oscillations. For example, in our simulation, 20% of the cases required more than one cycle for achieving proper selection. Oscillations, however, were not observed experimentally during SOP selection.

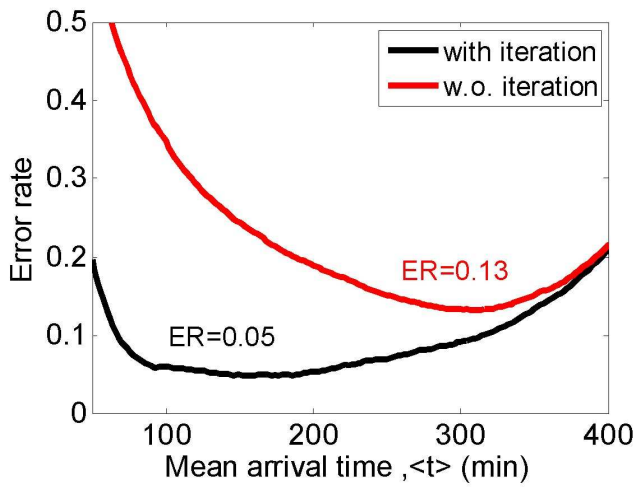

Supp Figure 2: Reduction of error rate in an iterative process. Error rates as function of the mean arrival time in a system that allow iteration (black) and a system without iteration (red). The minimal error rates are 4% and 14%, respectively. ER, error rate.

Section 6. Transcription-based feedback model of lateral inhibition process: the effective time delay, τ^{eff}

In this section, we describe the feedback-based model discussed in Figure 4A of the main text. We present its mathematical formulation and connect it to the abstract model considered in the Supplementary Section 1, by deriving the effective delay, τ^{eff}, as a function of the kinetic parameters in this model. This is done by approximating the dynamics analytically.

We consider the following components of the Notch-Delta network [3]:
A: achaete-scute, the proneural transcription factors whose expression defines the pro-neural cluster and enables the expression of Notch ligands. The selected SOP is marked by abundant achaete-scute.
D: Notch ligands, Delta and Serrate.
N: Notch receptor:

N^{ID}: Notch intracellular domain.
E: Notch targets genes of the Enhancer of Split [E(spl)] complex, which mediate all known Notch-dependent feedback mechanisms. In particular, E(spl) represses the proneural potential of Notch-activated cells.
R: Senseless, expressed downstream of the achaete-scute transcription factors, which represses the expression of E(spl) genes [4]. We assume that in this way, Senseless renders the cell refractory to Notch signaling.

We assume that all cells are equivalent, and that they all interact with one another in an equivalent way. Communication between the cells is mediated by the lateral binding of Delta to Notch. This binding generates the active form of Notch, the free Notch intracellular domain, N^{ID}, which drives the expression of E(spl). The reaction defining Notch activation is thus given by:

$$\text{(6. 1)}\quad D_i + N_j \underset{k^-}{\overset{a}{\rightleftharpoons}} \left[D_i N_j\right] \xrightarrow{k^+} N_j^{ID} + D_i ,$$

where we assumed that, following this cleavage, the ligands are recycled and can bind to additional Notch receptors [5]. Here, *i* and *j* are two cells in the cluster, and a, k^- and k^+ are the association, disassociation and complex cleavage rates, respectively, and the disassociation constant is defined as: $k_d = \dfrac{k^+ + k^-}{a}$.

The model is described by the following set of differential equations:

$$\text{(6. 2)}\quad \frac{dA_i}{dt} = \beta_A \frac{1}{\left(E_i/k_E\right)^{\upsilon} + 1} - \lambda_A A_i$$

$$\text{(6. 3)}\quad \frac{dR_i}{dt} = \beta_R \frac{1}{\left(k_A/A_i\right)^{\eta} + 1} - \lambda_R R_i$$

$$\text{(6. 4)}\quad \frac{dD_i}{dt} = \beta_D \frac{1}{\left(k_A/A_i\right)^{\eta} + 1} - \lambda_D D_i - aD_i \sum_{j\neq i} N_j + \left(k^+ + k^-\right) \sum_{j\neq i} \left[D_i N_j\right]$$

$$\text{(6. 5)}\quad \frac{dN_i}{dt} = \beta_N - \lambda_N N_i - aD_j \sum_{j\neq i} N_i + k^- \sum_{j\neq i} \left[D_j N_i\right]$$

$$\text{(6. 6)}\quad \frac{d\left[D_i N_j\right]}{dt} = aD_i N_j - \left(k^+ + k^-\right)\left[D_i N_j\right]$$

$$\text{(6. 7)}\quad \frac{dN_i^{ID}}{dt} = k^+ \sum_{j\neq i} \left[D_j N_i\right] - \lambda_{N^{ID}} N_i^{ID}$$

$$\text{(6. 8)}\quad \frac{dE_i}{dt} = \beta_E \frac{1}{1 + \left(k_{N^{ID}}/N_i^{ID}\right)^{\rho}} \frac{1}{1 + \left(R_i/k_R\right)^{\eta}} - \lambda_E E_i$$

β denote production rates, λ degradation rates, k dissociation constants, and υ, ρ and η are Hill parameters (defining the sharpness of the repression or induction functions).

The initial amounts of all components are set to zero, with the exception of Notch, which is set to the initial steady-state value: $N_0 = \frac{\beta_N}{\lambda_N}$.

To estimate the effective inhibition delay in this system, we first reduced this set of equations to a simplified single-component model, as described in the main text Methods. We define the ac/sc complex, *A*, as *M* in the single-component model. To this end, we considered the following simplifications:

1. All the interactions are non-linear, so that υ, ρ and η >>1. In this case, k_E, k_A, k_R and $k_{N^{ID}}$ set the thresholds for the activity of *E*, *A*, *R* and N^{ID}, respectively. Below this threshold, repression is negligible, whereas above this threshold downstream genes are fully repressed.
2. The thresholds for the activity of *E*, *A*, and *R* are much smaller than their maximal steady state levels: $k_i << \frac{\beta_i}{\lambda_i}$. This is assumed to facilitate rapid activation.
3. Notch-Delta interaction is at quasi-steady state, so that $d\left[D_i N_j\right]/dt \approx 0$, or

$$(6.\ 9)\ \left[D_i N_j\right] = \frac{D_i N_j}{k_d}\ ;\ \forall i, j \neq i\ .$$

Under these assumptions, the dynamics of the system can be divided into two parts: (1) *A* (ac/sc) accumulates in all cells, and (2) one cell (for instance Cell 1) is selected as a SOP and initiates lateral activation of Notch in all adjacent cells.

Our assumptions for mutually-interacting clusters of cells and the non-linearity in the cell-cell interactions enabled us to limit our below analysis to a cluster of only two interacting cells (the fastest two cells in the cluster). Based on those assumptions, the asymmetry between the two cells can be modeled as a time-difference, Δt, in the initiation of *A* production. We neglect any other differences between the cells for instance, differences resulting from stochastic fluctuations in the production and degradation of A. This simplification greatly facilitates the theoretical analysis but does not limit generality because it is fully equivalent to any other type of stochastic process.

During the initial part of the dynamics, prior to reaching the threshold, the amount of *A* is given by solving Eq. 6.2:

$$(6.\ 10)\qquad A_1(t) = \frac{\beta_A}{\lambda_A}\left(1 - \exp^{-\lambda_A t}\right) \text{ and}$$

$$(6.\ 11)\qquad A_2(t) \underset{t>\Delta t}{=} \frac{\beta_A}{\lambda_A}\left(1 - \exp^{-\lambda_A (t-\Delta t)}\right)$$

The first cell to be selected, Cell 1, initiates lateral inhibition at time t_1^{in}, which is defined by the selection threshold, k_A:

(6. 12) $$t_1^{in} = \frac{1}{\lambda_A}\log\left(\frac{\beta_A/\lambda_A}{\beta_A/\lambda_A - k_A}\right) \underset{k_A << \frac{\beta_A}{\lambda_A}}{\sim} \frac{k_A}{\beta_A}$$

And clearly:

(6. 13) $$t_2^{in} = t_1^{in} + \Delta t$$

We assume that once the cell has reached this threshold (t_1^{in}), it begins to accumulate senseless (R_1). This cell will become refractory when R reaches the threshold abundance at which R represses E: k_R. Accordingly, the time for reaching refractoriness is given by:

(6. 14) $$t_1^r \sim t_1^{in} + \frac{k_R}{\beta_R}$$

Considering the selection rule, Eq. 1.1 and 1.3, we can thus define one component of the effective delay:

(6. 15) $$t_i^r - t_i^{in} = \frac{k_R}{\boldsymbol{\beta}_R} \equiv \boldsymbol{\tau}^R .$$

Next, we estimate the selection delay, τ^s (the delay from the onset of lateral signaling in cell 1 until the SOP potential of cell 2 is inhibited). In the present model, such inhibition requires that the Notch signal will propagate to prevent the auto-activation of the ac/sc complex, A. To estimate this time, we consider the second part of the system dynamics, following the initiation of lateral inhibition by one of the cell.

This second stage begins at time t_1^{in}. At this time, D_1 begins to accumulate, so that its abundance at $t > t_1^{in}$ is given by:

(6. 16) $$D^{tot}{}_1(t) = \frac{\beta_D}{\lambda_D}\left(1 - \exp^{-\lambda_D (t - t_1^{in})}\right).$$

This accumulating D interacts with Notch in the adjacent cell and generates N^{ID} according to (Eq. 6.7):

(6. 17) $$\dot{N}_2^{ID}(t) = k^+ D_1^{tot} \frac{N_2}{k_d + N_2} - \lambda_{N^{ID}} N_2^{ID}$$

Assuming fast degradation of N^{ID} (relative to the changes in D^{tot}) we get

$$(6.18) \qquad N_2^{ID}(t) \approx \frac{k^+ D_1^{tot}\left(t - 1/\lambda_{N^{ID}}\right)}{\lambda_{N^{ID}}} \frac{N_2}{k_d + N_2} .$$

Thus, the amount of N^{ID} at time t is proportional to the amount of D^{tot} in the neighboring cell at an earlier time, $t - 1/\lambda_{N^{ID}}$. The first contribution to the selection delay is thus $1/\lambda_{N^{ID}}$.

The second contribution to the selection delay is the time required for D to reach abundance that will generate sufficient N^{ID} to activate target genes. Such activation will begin when N^{ID} reaches the threshold abundance, $N^{ID} = k_{N^{ID}}$, and will require D to reach the critical level:

$$(6.19) \qquad k_D^{eff} = \frac{k_{N^{ID}} \boldsymbol{\lambda}_{N^{ID}}}{k^+} \frac{k_d + N_2}{N_2}$$

This will cause an additional delay that is estimated by:

$$(6.20) \qquad \tau^D \sim \frac{k_D^{eff}}{\beta_D} .$$

Finally, an additional delay is introduced by the need to accumulate sufficient E to inhibit A. Following similar considerations as above, this delay is estimated as:

$$(6.21) \qquad \tau^E = \frac{k_E}{\beta_E} .$$

Together, the overall selection delay is:

$$(6.22) \qquad \boldsymbol{\tau}^s = 1/\boldsymbol{\lambda}_{N^{ID}} + \boldsymbol{\tau}^D + \boldsymbol{\tau}^E .$$

The rules for successful selections for the refractoriness scenario, as given by Eq. 1.1 and 1.3: can now be written using Eq. 6.15 and 6.22 as:

$$(6.23) \qquad \Delta t > 1/\boldsymbol{\lambda}_{N^{ID}} + \boldsymbol{\tau}^D + \boldsymbol{\tau}^E - \boldsymbol{\tau}^R = \boldsymbol{\tau}^{eff} .$$

$$(6.24) \qquad \boldsymbol{\tau}^{eff} = 1/\boldsymbol{\lambda}_{N^{ID}} + \frac{k_D^{eff}}{\boldsymbol{\beta}_D} + \frac{k_E}{\boldsymbol{\beta}_E} - \frac{k_R}{\boldsymbol{\beta}_R}$$

We note that all the delays: $\boldsymbol{\tau}^D, \boldsymbol{\tau}^E$, and $\boldsymbol{\tau}^R$ involve transcriptional and translational processes. These are quite lengthy, particularly the initiation and elongation steps of transcription, which have a time scale of at least ~10min [6]. Moreover, transcriptional

and translational events are uncoupled from each other and noisy, and we thus do not favor the theoretical possibility of minimizing τ^{eff} by fine-tuning these different delays.

In conclusion, we estimate the effective delay to be at least as long as the typical time associated with transcription initiation and elongation:

$$\tau^{eff} > 10\,\text{min} \tag{6. 25}$$

Alternative models that set the threshold for selection at different points in the lateral-inhibition circuits (other than the ac/sc abundance assumed here) can be analyzed in a similar manner. None of these models is capable of producing a lower effective delay than 10 min because to the need to induce E(spl). For example, even if the threshold for selection and inhibition is defined by the time it takes to activate Neuralized, this still requires accumulation of E(spl) and will consequently be delayed by $\tau^{E} \sim 10\,\text{min}$.

Section 7. Cis inhibition model of lateral inhibition process: the effective time delay, τ^{eff}

In this section, we describe the extended lateral-inhibition model that includes the cis interaction between Notch and its ligands, Delta and Serrate, as discussed in the main text, Figure 4B. We present its mathematical formulation and provide the parameters used in our simulation, shown in Figure 4D. We then connect it to the abstract model considered in the Supplementary Section 1, by deriving the effective delay, τ^{eff}, as a function of the kinetic parameters in this model. This is done by approximating the dynamics analytically.

The extended model includes two types of interactions between Notch and its ligands Delta and Serrate: Lateral inhibition, which generates an active cleavage product, N^{ID}, and cell autonomous interaction which does not generate, N^{ID}. Specifically,

<u>Interaction in trans:</u>

$$D_i + N_j \underset{k_1^-}{\overset{a_1}{\rightleftharpoons}} \left[D_i N_j \right] \xrightarrow{k_1^+} N_j^{ID} + D_i \tag{7. 1}$$

<u>Interaction in cis:</u>

$$D_i + N_i \underset{k_2^-}{\overset{a_2}{\rightleftharpoons}} \left[D_i N_i \right] \xrightarrow{k_2^+} D_i \tag{7. 2}$$

Here, $a_1, k_1^-, k_1^+, a_2, k_2^-, k_2^+$ are the association, dissociation and complex cleavage rates for the trans and cis interaction, respectively, as shown in Eqs. 7.1 and 7.2. The disassociation constants are given by $k_d^{trans} = \frac{k_1^+ + k_1^-}{a_1}; k_d^{cis} = \frac{k_2^+ + k_2^-}{a_2}$.

We assume that $k_i^- \to 0$, and that $a_2 >> a_1$ so that the cis interaction dominates: $k_d^{cis} << k_d^{trans}$.

As described in the main text, cells in this model become refractory through the ligand-dependent depletion of free Notch. We thus simplify the system by not considering explicitly the dynamics of Senseless and of the ac-sc transcription complex.

Adding the cis interaction Eq. 7.2 into the model we obtain the following set of differential equations:

(7. 3) $$\frac{dD_i}{dt} = \beta_D \frac{1}{\left(E_i / k_E\right)^{\upsilon} + 1} - \lambda_D D_i - a_2 D_i N_i + k_2^+ \left[D_i N_i\right] - a_1 D_i \sum_{j \neq i} N_j + k_1^+ \sum_{j \neq i} \left[D_i N_j\right]$$

(7. 4) $$\frac{dN_i}{dt} = \beta_N - \lambda_N N_i - a_2 D_i N_i - a_1 N_i \sum_{j \neq i} D_j$$

(7. 5) $$\frac{dN_i^{ID}}{dt} = k_1^+ \sum_{j \neq i} \left[D_j N_i\right] - \lambda_{N^{ID}} N_i^{ID}$$

(7. 6) $$\frac{dE_i}{dt} = \beta_E \frac{1}{1 + \left(k_{N^{ID}} / N_i^{ID}\right)^{\rho}} - \lambda_E E_i$$

(7. 7) $$\frac{d\left[D_i N_i\right]}{dt} = a_2 D_i N_i - k_2^+ \left[D_i N_i\right]$$

(7. 8) $$\frac{d\left[D_i N_j\right]}{dt} = a_1 D_i N_j - k_1^+ \left[D_i N_j\right]$$

β denote production rates, λ degradation rates, k dissociation constants and υ and ρ are Hill coefficients. The initial levels of all components are set to zero, with the exception of Notch, whose level is set to the initial steady-state value: $N_0 = \frac{\beta_N}{\lambda_N}$.

Model simulations and parameters:

As described in the main text, the dynamics of the system can be divided into three parts. First, the ligands, *D*, accumulate within each cell, gradually depleting free Notch by facilitating endocytosis or by simply binding to it. This accumulation is stochastic and occurs in each cell independently. Once free intracellular Notch had been depleted in one of the cells, the ligands can bind Notch in adjacent cells, generating a pulse of N^{ID} in

these lateral cells. Finally, this initial pulse of N^{ID} generates the conditions for sustained repression. Sustained repression follows because, after the initial pulse of N^{ID}, the ligand concentrations are reduced in the repressed cell, enabling re-accumulation of the Notch receptor. Stochasticity does not play a major role in these two latter processes.

This separation of the dynamics into two stages – one that relies on stochastic differences between the cells and a second that is deterministic - greatly simplify the numerical simulations by enabling us to treat each of the stages separately, including stochastic effects only at the first stage, and following deterministic dynamics in the second and the third stages. More specifically, we assume that stochasticity has a role only in determining the time at which free Notch is eliminated, namely the time difference when lateral inhibition would have been initiated by two independent cells, t_1^{in} and $t_2^{in}: \Delta t = t_2^{in} - t_1^{in}$ (as defined in Supplementary Section 1 above). The numerical simulations reported in the text (Figure 4C-D) were thus performed by solving Equations 7.3-7.8 numerically, assuming a stochastic difference, Δt in the initiation times of *D* production by the cells.

The effective inhibition delay is defined as the minimal time that is required to activate Notch in order to ensure the eventual repression of the cell. We derive this effective delay indirectly, by measuring the minimal time-difference Δt (between the first and the second cell to initiate their *D* production) which still provides proper selection. This minimal difference is the same as the effective delay $\boldsymbol{\tau}^{eff} = \Delta t_{\min}$.

An analytical solution of the model (below) indicates that the error-rate depends on ratios of parameters, rather than on their absolute values. Most of the parameters in the model have not yet been measured, certainly not in vivo. We thus set the value of a subset of the parameters based on plausible biological regimes, and predict the corresponding values of few parameters based on the analytical insights gained from the analysis below.

The following parameters were used in the simulations reported in main text:

1. *Half lives*: we assume a half life of 100min for Notch, Delta, and E(spl) protein: so that $\lambda_N, \lambda_D, \lambda_E = \frac{1}{100}\min^{-1}$. A 10min half life is assumed for N^{ID}, $\lambda_{N^{ID}} = \frac{1}{10}\min^{-1}$ [7].
2. *Concentrations*: protein concentrations are given in molecules/cell. Since the volume of the proneural cluster cells is ~100μm^3, ~50,000 molecules are equivalent to 1μM. We estimate a constant production rate of 200 Notch receptors per minute ($\beta_N = 200\, molecule/\min$), corresponding to a steady state abundance (before ligand production) of N_0 =20,000 receptor per cell. Delta production rate was taken as $\beta_D = 50 molecules / \min$ in order to scale Notch elimination timing to ~120min.
3. *DNA binding*: an essential assumption is that N^{ID} is active at very low concentrations. This assumption is supported by experiments showing that very small amounts of N^{ID}, below the immunofluorescence detection level, are active [8]. Specifically, we

assume $k_{N^{ID}} = 20 molecules$. The association constant of E(spl) was calibrated to enable E(spl) activation upon N^{ID} pulse: $\frac{k_E}{\beta_E} \sim \frac{1}{\lambda_{N^{ID}}} = 10\,\text{min}$.

4. *Hill coefficients*: $\rho = \nu = 2$.
5. *Notch-Delta trans interaction*: we consider $k_1^+ = 1\,\text{min}^{-1}$ as the cleavage rate of the Notch-Delta complex, and a trans association constant of is $a_1 = 1\,\text{min}^{-1}$ (corresponding to ~0.01nM^{-1} min^{-1}, using scaling factor of 100 for Notch and Delta concentration on the cell membrane).
6. *Notch-Delta cis interaction:* $a_2 = 1000\,\text{min}^{-1}$ as the association constant in cis and $k_2^+ = 0.1\,\text{min}^{-1}$ as dissociation constant in cis.

Defining the selection rule in the cis-interaction model:
One of the key characteristics of the cis-inhibition model is that the initiation of lateral signaling is concomitant with the onset of refractoriness. Accordingly, $t_i^r - t_i^{in} = 0$, and the selection rule, Eq. 1.1 and Eq. 1.3 is reduced to:

$$\Delta t > \boldsymbol{\tau}^s .$$

$\boldsymbol{\tau}^s$ may be shorter than when not considering cis interactions because refractoriness prevents sensing Notch activation, but does not prevent SOP inhibition by N^{ID} if this cleaved form of Notch is already present in the cell. More specifically, N^{ID} or E(spl) can still inhibit ac/sc auto-activation and prevent SOP selection, even in cells that have become refractory to lateral signaling because their Notch receptors are fully saturated. Consequently, generation of a signal that will eventually inhibit SOP selection does not require accumulation of E(spl). As we describe below, the potential to become an SOP can be prevented by a pulse of N^{ID} generated prior to the elimination of free Notch in the inhibited cell.

Analytical approximation
In the following analysis, we approximate the dynamics defined by the present cis-based model. Using this approximation, we estimate the effective time delay τ^{eff}.

Without loss of generality, we will describe a cluster of two interacting cells, representing the fastest two cells form the *n* cells cluster.

We assume that the complexes are at quasi-steady state, so that $[D_i N_i] = \frac{D_i N_i}{k_d^{cis}}$ and $[D_i N_j] = \frac{D_i N_j}{k_d^{trans}}$. As before, from Eq. (7.3-7.8) we obtain:

$$\frac{dD_i^{tot}}{dt} = \beta_D \frac{1}{(E_i/k_E)^{\upsilon} + 1} - \lambda_D D_i^{tot} \tag{7. 9}$$

and

(7. 10) $D_i = D_i^{tot} \Big/ \left(1 + \frac{N_i}{k_d^{cis}} + \frac{N_j}{k_d^{trans}}\right)$.

Notch is endocytosed following its interaction with Delta, so that its concentration is continuously reduced. Initially, when Notch concentrations are sufficiently high, interaction in cis dominates. Later, when Notch has been eliminated from one of the cells, interaction in trans starts playing a role. We analyze separately these two stages of the system dynamics.

Stage I: prior to reaching threshold

First, we examine the dynamics of the system before Notch is eliminated. We assume that at this stage the concentration of *N* and *D* are similar in both cells.

Because in the presence of Notch, $\frac{k_d^{trans}}{k_d^{cis}} \underset{N_j \sim N_i}{>>} \frac{N_j}{N_i}$, we can write:

(7. 11) $D_i \approx D_i^{tot} \frac{k_d^{cis}}{k_d^{cis} + N_i}$

and

(7. 12) $\dot{N}_i(t) = \beta_N - \lambda_N N_i - k_2^+ D_i^{tot} \frac{N_i}{k_d^{cis} + N_i} - k_1^+ D_j^{tot} \frac{k_d^{cis}}{k_d^{trans}} \frac{N_i}{k_d^{cis} + N_i}$,

Throughout most of this stage, the dynamics of Notch can be further approximated as:

(7. 13) $\dot{N}_i(t) \sim \beta_N - \lambda_N N_i - k_2^+ D_i^{tot}$

Thus, in order for Notch to be fully eliminated it is necessary that

(7. 14) $k_2^+ D_i^{tot} > \beta_N$.

If this doesn't hold, the system may reach a steady state with constant concentration of *N* and *D*, in which case no selection will occur.

At this stage, in addition to the interaction in cis, a minor interaction in trans between Notch and Delta occurs. Thus, D^{tot} in one cell depends on D^{tot} in the adjacent cell. Next, we derive the conditions under which Notch is fully eliminated by its ligands.

To estimate D_i^{tot}, we first approximate N_i^{ID}. From Eq. 7.5 we obtain:

(7. 15) $\dot{N}_i^{ID}(t) = k_1^+ D_j^{tot} \frac{k_d^{cis}}{k_d^{trans}} \frac{N_j}{k_d^{trans} + N_j} - \lambda_{N^{ID}} N_i^{ID}$.

Assuming a quasi-steady state, this can be further reduced to

(7. 16) $N_i^{ID}(t) \approx \frac{k_1^+ D_j^{tot}\left(t - 1/\lambda_{N^{ID}}\right)}{\lambda_{N^{ID}}} \frac{k_d^{cis}}{k_d^{trans}}$.

Using similar approximations, we can also estimate E_i

(7. 17) $E_i(t) \approx \frac{\beta_E}{\lambda_E}\left(\frac{N_i^{ID}\left(t - 1/\lambda_E\right)}{k_{N^{ID}}}\right)^2 = \frac{\beta_E}{\lambda_E}\left(\frac{k_1^+ D_j^{tot}\left(t - 1/\lambda_{N^{ID}}\right)}{k_{N^{ID}}\lambda_{N^{ID}}} \frac{k_d^{cis}}{k_d^{trans}}\right)^2$.

Using Eq. 7.9, $D_{\min}^{tot}$ which is the minimal Delta concentration for the full elimination of free Notch Eq. 7.14 above can now be written as

(7. 18) $D_{\min}^{tot} \sim \frac{\beta_D}{\lambda_D} \frac{1}{1 + \left(E_{\min}/k_E\right)^2}$,

which can be further written as (using Eq. 7.14):

(7. 19) $E_{\min} \sim k_E \sqrt{\frac{\beta_D}{\lambda_D} \frac{k_2^+}{\beta_N} - 1}$.

Substituting Eq. 7.19 back in Eq. 7.17 we get the condition required for free Notch to be fully eliminated by its ligands:

(7. 20) $\left(\frac{k_d^{cis}}{k_d^{trans}}\right)^2 < \frac{\lambda_E k_E}{\beta_E}\left(\frac{\lambda_{N^{ID}} k_{N^{ID}} k_2^+}{\beta_N k_1^+}\right)^2 \sqrt{\frac{\beta_D}{\lambda_D} \frac{k_2^+}{\beta_N} - 1}$.

Note that a dominant cis interaction, $\frac{k_d^{cis}}{k_d^{trans}} << 1$ is required for conditions (7.19) to hold.

Stage II and III: Lateral inhibition

The second stage of the dynamics is initiated when free Notch is fully eliminated in one of the cells (e.g "Cell 1”). At this time, *D* starts binding *N* in trans. This trans binding proceeds at a rate, κ^{trans} and generates a pulse of activated Notch, N_2^{ID} in the second cell**.** A pulse is generated because after some time, Δt, Notch will also be eliminated from the second cell, and this cell will become refractory to lateral activation by *D* from the first cell. The pulse size is determined by this time difference, Δt. The minimal time required to produce sufficient N^{ID} to lead to the eventual repression of the SOP state defines the effective inhibition delay, τ^{eff} in this system.

We calculate τ^{eff} as follows. We consider the limiting case where the peak concentration of the N_2^{ID} pulse is obtained at time $t^{in}+\tau^{eff}$ and demand that this pulse will be just sufficient to repress the SOP fate. Specifically, if the peak of the pulse is achieved at time $t^{in}+\tau^{eff}$ then the peak concentration of N_2^{ID} will be given by:

(7. 21) $N_2^{ID^P} = N_2^{ID}\left(t^{in}+\tau^{eff}\right) \sim \tau^{eff}\kappa^{trans}$

In this calculation, we assume that both τ^{eff} as well as the typical time characterizing Notch processing in trans ($1/k_1^+$) are fast compared to the degradation rate of N^{ID}, such that all of the *trans*-bound Notch contribute to the generation of N^{ID}.

The concentration of N_2^{ID} will then begins to decay, such that at any subsequent time *t* it will be given by:

(7. 22) $N_2^{ID}\left(t^{in}+\tau^{eff}+t\right) = N_2^{ID^P}\exp(-\lambda_{N^{ID}}t)$.

This activated Notch will continue to activate the down-stream gene *E*, as long as its concentration are higher than the threshold $k_{N^{ID}}$. The time in which E will be activated (t^p, effective pulse width) is that given by:

(7. 23) $t^p = \frac{1}{\lambda_{N^{ID}}}\log\left(N_2^{ID^P}/k_{N^{ID}}\right) = \frac{1}{\lambda_{N^{ID}}}\log\left(\tau^{eff}\kappa^{trans}/k_{N^{ID}}\right)$

In order to ensure repression of the SOP fate, the pulse of *E* that follows the generation of N^{ID} should reduce D_2^{tot} to below the minimal level required to eliminate Notch in cis (Eq. 7.19). If this, in fact, occurs, a subsequence pulse of N_2^{ID} will follow, allowing Notch to reaccumulate. This re-accumulation will lead to the final repression of the second cell. From Eq. 7.6 (assuming $\lambda_{N^{ID}} > \lambda_E$ and $\frac{k_d^{cis}}{k_d^{trans}} << 1$), we estimate the concentration of the *E* pulse that will be generated by:

(7. 24) $E_2^p \sim \frac{\beta_E}{\lambda_{N^{ID}}}\log\left(\tau^{eff}\kappa^{trans}/k_{N^{ID}}\right)$.

Together with Eq. 7.19, this sets the condition for proper selection as

(7. 25) $\frac{\beta_E}{\lambda_{N^{ID}}}\log\left(\tau^{eff}\kappa^{trans}/k_{N^{ID}}\right) > k_E\sqrt{\frac{\beta_D}{\lambda_D}\frac{k_2^+}{\beta_N}-1}$

From this, we can estimate the effective time delay, τ^{eff}:

(7. 26) $\tau^{eff} \sim \frac{k_{N^{ID}}}{\kappa^{trans}} \exp\left(\frac{\lambda_{N^{ID}} k_E}{\beta_E} \sqrt{\frac{\beta_D}{\lambda_D} \frac{k_2^+}{\beta_N} - 1} \right).$

Eq. 7.26 and Eq. 7.20 set the constraints that model parameters need to satisfy in order to ensure short inhibition delay.

Section 8. Predicted error rates for different combinations of Notch, Delta, and Serrate heterozygotes

In this section we predict the error rate in flies of different heterozygote backgrounds, based on the models described in Sections 6 and 7 (with or without potent interaction in cis). We show that these models generate distinct predictions regarding the interaction between Notch and Delta. As discussed in the main text, experimental data of the error rates favor the cis interaction model.

To model heterozygote backgrounds, we halve the production rates, taking the relevant $\boldsymbol{\beta} \to \frac{1}{2}\boldsymbol{\beta}$, and keeping all the other parameters unchanged. We then calculate numerically the change in the effective inhibition delay, τ^{eff}, and the mean arrival time <t>. We assume that the noise degree (α) remain the same so that the width of the arrival time distribution is maintained at 50min for all tested backgrounds. The specific noise degree in the process controls the absolute values of the predicted error rates, but has little effect on their relative values. The key factor regulating the difference in the error rates is the change in the effective time delay. Having the effective inhibition delay and noise, we use Eq. 2.5, Section 2, to predict the error rate.

Cis-interaction model

Qualitatively, using the analytical approximations derived in Section 7, we note that τ^{eff} depends on the production rates of Notch and Delta through their effect on the exponent term in Eq. 7.26 which depends on: $\frac{\beta_D}{\beta_N}$.

Accordingly, Notch heterozygosity ($\beta_N \to \frac{1}{2}\beta_N$) will increase the effective inhibition delay, while heterozygosity for Delta/Serrate ($\beta_D \to \frac{1}{2}\beta_D$) will decrease this delay. Combined heterozygosity for Notch and Delta/Serrate will have a compensatory effect.

For a quantitative estimation that also takes into account the dependence of Notch activation pulse on Notch and Delta production rates, we simulated Eq. 7.3-7.8 with

perturbed production rates. We validated that the obtained inhibition delays and mean arrival times fit the analytical approximations.

Experimentally, we observed the predicted compensation when Notch heterozygous is combined with Serrate heterozygous (main text Figure 5A and Supp. Table 1). Compensation is not observed when Notch heterozygous is combined with Delta heterozygous, suggesting asymmetric roles for the Notch ligands Delta and Serrate. We modeled this by splitting Delta/Serrate (D) in Eq. 7.3-7.8 into two distinct components D and S and assuming that Serrate can interact with Notch only in cis, whereas Delta can interact with Notch in both cis and trans. We thus removed Eq. 7.4 from the model and introduced the following three equations in its place:

$$\text{(8. 1)} \quad \frac{dN_i}{dt} = \beta_N - \lambda_N N_i - a_2 D_i N_i - a_2 S_i N_i - a_1 N_i \sum_{j \neq i} D_j$$

$$\text{(8. 2)} \quad \frac{dS_i}{dt} = \beta_S \frac{1}{\left(E_i / k_E\right)^{\upsilon} + 1} - \lambda_S S_i - a_2 S_i N_i + k_2^{+} \left[S_i N_i\right]$$

$$\text{(8. 3)} \quad \frac{d\left[S_i N_i\right]}{dt} = a_2 S_i N_i - k_2^{+} \left[S_i N_i\right]$$

Using this extended system, we evaluated numerically the inhibition delay and mean arrival times, as reported in main text Figure 5B-D. We used the same procedure and parameters as reported in Section 7 ("Model simulation and parameters"), but with the following adjustments:
$\beta_D = 25 molecules / \min$, $\beta_S = 20 molecules / \min$ and $a_2 = 500 \min^{-1}$.

Prediction of error rates for the feedback model (without cis **interaction)**
We repeated the same analysis for the feedback model. The production rate of Notch and Delta will influence the effective inhibition delay, τ^{eff}, by changing one of its components, τ^D, defined in Eq. 6.19-6.20: $\boldsymbol{\tau}^D = \frac{1}{\boldsymbol{\beta}_D} \frac{k_{N^{ID}} \boldsymbol{\lambda}_{N^{ID}}}{k^+} \frac{k_d + \boldsymbol{\beta}_N / \boldsymbol{\lambda}_N}{\boldsymbol{\beta}_N / \boldsymbol{\lambda}_N}$.

The feedback model can thus explain the increased error rate for Notch heterozygous if we assume that $k_d >> \boldsymbol{\beta}_N / \boldsymbol{\lambda}_N$, in which case $\boldsymbol{\tau}^D \propto \frac{1}{\boldsymbol{\beta}_D \boldsymbol{\beta}_N}$. In this case, reducing Notch production rate will increase the delay τ^{eff}, leading to a higher error rate. However, the model will predict an increase (rather than a decrease) in the effective delay for heterozygosity for Delta and Serrate, leading to a higher error rate in these heterozygotes. Moreover, combining heterozygosity for Delta/Serrate with that for Notch is predicted to be additive, and not compensating.

Section 9. A smooth inhibition function leads to a higher error rate

Throughout our analysis, we modeled lateral inhibition as a step-like function, implying that the cells are basically independent before one of them reaches the inhibition threshold. In actuality, we expect inhibition to increase gradually, although (as was also shown in other studies) non-linearity of inhibition is essential for selection. (In the case of linear inhibition, the two cells will attain a common – intermediate – state, and no selection will ensue). In this section, we used numerical simulations to examine whether a smooth inhibition function could lead to a lower error rate. Instead, we found that error rate increases when non-linearity decreases. This justifies our choice of a threshold-like inhibition as a means for calculating the minimal possible error rate.

We simulated a smooth inhibition function by replacing the θ function in Eq. M.2 (Methods) by a Hill function, with the parameter υ describing the degree of non-linearity:

(9. 1) $$f(M_i, M_j, t) = \frac{1}{1+\left(M_j\left(t-\tau^{in}\right)/k^{in}\right)^{\upsilon}}$$

Clearly, the system becomes more threshold-like with increasing υ. We also decided to simulate the scenario allowing iterations, as this provides the lowest possible error, and thus did not include refractoriness. We used the same parameters as in main text Methods.

The simulation results are summarized in fig. S3, depicting the error rate as a function of the Hill coefficient. Here, a selection process is defined as successful if during the available time window (taken here to be T=360min) one, and only one cell reached M_i abundance that is above the threshold for irreversible selection, k^s. Clearly, the minimal error is obtained for high Hill-coefficients, corresponding to the threshold-like inhibition considered in our analysis.

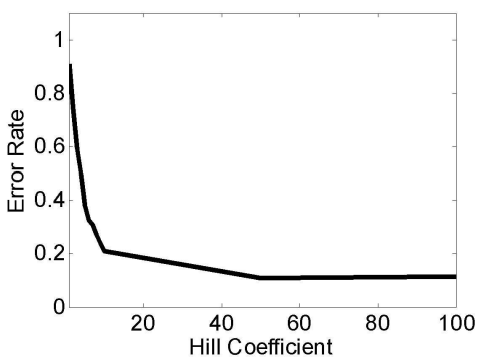

Supp Figure 3: Simulation results showing the error rates as a function of the Hill coefficient (measuring the extent of non-linearity). The stochastic single-component model described in main text Methods was used.

Section 10. Validation for the use of the mα reporter

A possible drawback of in-vivo imaging is that endogenous markers for the selected SOP cell are lacking. In fact, we identified the selected SOP as a non-repressed cell (positive for ubi-NLS-GFP and negative for E(spl)mα-DsRed.T4-NLS marking) within the proneural cluster. This indirect detection method is based on reporter reliability ; here, we substantiate the use of E(spl)mα-DsRed.T4-NLS for SOP identification.

Castro *et. al*. [9] characterized the mα reporter and found that its activation depended on the Notch intracellular domain and pro-neural transcription factors (such as ac-sc). Thus, the mα reporter is a marker for Notch activation within the pro-neural cluster.

In the same work, mα reporter expression was complementary to that of Hnt, a SOP marker [9].

To verify the reliability of SOP identification based on lack of mα reporter expression, we independently co-stained discs for Senseless, an established SOP marker [10] and the mα-reporter. The expression patterns of Senseless and the mα-reporter were mutually exclusive in all the pro-neural clusters we analyzed (>100 clusters). An example of the detection pattern of Senseless and the mα-reporter is given in fig. S4A.

Consistent with the in-vivo imaging, we observed occasional cases where two adjacent cells expressed Senseless, but not the mα-reporter (see fig. S4B). We could not identify any case in which a cell did not express Senseless, while being surrounded with cells expressing the mα-reporter. Together this data support the reliability of using mα-reporter for detecting double selection.

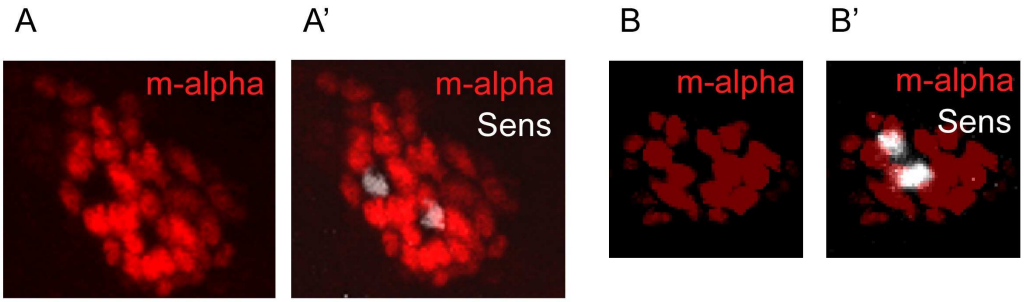

Supp Figure 4: Validation of SOP detection using the mα reporter A) pro neural cluster in the imaginal disc of the control fly strain *hsflp; E(spl)mα-DsRed.T4-NLS;FRT80B, ubi-NLS-GFP*, stained for Senseless (white, A') as a marker for SOP, mα reporter expressing cells (red) mark the non-selected cells. B) Error in SOP selection. Duplicated SOP selection of adjacent cells (stained for Senseless, white, B') was identified in imaginal disc of Notch heterozygous (N^{55e11},FRT101/hsflp,FRT101,cGFP; mα-dsRED) flies.

Name	**Genotype: (male X female)**	**Flies #**	**aSC bristles ectopic selection error rate**
OregonR	OregonR	246	0.4% (2/492)
Yellow White (y.w)	y.w.	202	0.8% (3/404)
CantonS	CantonS	126	11% (28/252)
Control	CantonS X y.w	57 (female)	0.9% (1/114)
Notch het.	y.w. X N^{55e11},FRT101	27 (female)	28% (15/54)
Serrate het.	Ser^{RX82}, FRT82B X y.w	31 (female)	0% (0/62)
Delta het.	Dl^{RevF10}, FRT82B X y.w	62 (female)	10% (13/124)
Delta-Serrate het. *	Dl^{RevF10}, FRT82B X Ser^{RX82}, FRT82B	16 (female)	12.5% (4/32)
Delta-Serrate het. **	Dl^{RevF10}, Ser^{RX82},FRT82B X y.w	48 (female)	0% (0/96)
Notch-Delta-Serrate het.	N^{55e11},FRT101 X Dl^{RevF10}, Ser^{RX82}, FRT82B	47 (female)	0% (0/94)
Notch-Delta het.	N^{55e11},FRT101 X Dl^{RevF10}, FRT82B	33 (female)	26% (17/66)
Notch-Serrate het.	N^{55e11},FRT101 X Ser^{RX82}, FRT82B	47 (female)	13% (12/94)

Supp. Table 1: Summary of the specific genotypes tested for ectopic selection of anterior scutellar (aSC) bristles. Because Notch (located on X chr) heterozygous flies are female, only female adult flies were compared. The number of error vs. number of clusters is given in parentheses (two clusters for every fly). Note the difference in the observed error rates between * and **, both strains are Delta-Serrate heterozygous (* by crossing Delta and Serrate mutant alleles, and ** by using a recombinant allele of Delta and Serrate (Bloomington Stock Center)). Het., heterozygous.

References:

1. Collier, J.R.M., N. A.Maini, P. K.Lewis, J. H., *Pattern formation by lateral inhibition with feedback: a mathematical model of delta-notch intercellular signalling.* J Theor Biol, 1996. **183**(4): p. 429-46.
2. Plahte, E., *Pattern formation in discrete cell lattices.* J Math Biol, 2001. **43**(5): p. 411-45.
3. Fortini, M.E., *Notch signaling: the core pathway and its posttranslational regulation.* Dev Cell, 2009. **16**(5): p. 633-47.
4. Jafar-Nejad, H.A., M.Nolo, R.Lacin, H.Pan, H.Parkhurst, S. M.Bellen, H. J., *Senseless acts as a binary switch during sensory organ precursor selection.* Genes Dev, 2003. **17**(23): p. 2966-78.
5. Chitnis, A., *Why is delta endocytosis required for effective activation of notch?* Dev Dyn, 2006. **235**(4): p. 886-94.
6. Mier-y-Teran-Romero, L., M. Silber, and V. Hatzimanikatis, *The origins of time-delay in template biopolymerization processes.* PLoS Comput Biol. **6**(4): p. e1000726.
7. Gupta-Rossi, N.L.B., O.Gonen, H.Brou, C.Logeat, F.Six, E.Ciechanover, A.Israel, A., *Functional interaction between SEL-10, an F-box protein, and the nuclear form of activated Notch1 receptor.* J Biol Chem, 2001. **276**(37): p. 34371-8.
8. Schroeter, E.H., J.A. Kisslinger, and R. Kopan, *Notch-1 signalling requires ligand-induced proteolytic release of intracellular domain.* Nature, 1998. **393**(6683): p. 382-6.
9. Castro, B.B., S.Bailey, A. M.Posakony, J. W., *Lateral inhibition in proneural clusters: cis-regulatory logic and default repression by Suppressor of Hairless.* Development, 2005. **132**(15): p. 3333-44.
10. Nolo, R., L.A. Abbott, and H.J. Bellen, *Senseless, a Zn finger transcription factor, is necessary and sufficient for sensory organ development in Drosophila.* Cell, 2000. **102**(3): p. 349-62.